Sequence-Selective DNA Recognition and Photocleavage: A Comparison of Enantiomers of $Rh(en)_2phi^{3+}$ †

Thomas P. Shields and Jacqueline K. Barton*

Division of Chemistry and Chemical Engineering, California Institute of Technology, Pasadena, California 91125

Received June 13, 1995; Revised Manuscript Received August 25, 1995⊗

ABSTRACT: The recognition and photoinduced cleavage of DNA by the enantiomers of bis(ethylenediamine)-(9,10-phenanthrenequinone diimine)Rh(III) [$Rh(en)_2phi^{3+}$] have been characterized and the basis for enantioselective differences delineated. $Rh(en)_2phi^{3+}$ isomers bind strongly to DNA via intercalation and, upon photoactivation with near-UV light, produce direct strand cleavage. On the basis of product analysis, the photoinduced DNA cleavage appears to proceed by a mechanism consistent with that observed for the parent $Rh(phen)_2phi^{3+}$, involving direct abstraction of the 3′-hydrogen atom of the deoxyribose by the activated, intercalated phi. Quantitative photocleavage titrations indicate tight binding by both enantiomers to the DNA duplex. For Δ-$Rh(en)_2phi^{3+}$, DNA site affinities range from 0.3×10^6 to 8.0×10^6 M^{-1}, and a distinct preference for GC sites is evident. Λ-$Rh(en)_2phi^{3+}$ is found to be sequence neutral with an average site affinity of 2×10^6 M^{-1}. The basis for sequence selectivity of the enantiomers has been examined through comparison of photocleavage patterns to those of several phi complexes of rhodium(III) containing or lacking axial amines; those complexes containing the axial amines are found to target GC sites. DNA photocleavage studies on oligonucleotides containing the modified bases O^6-methylguanine, 7-deazaguanine, and deoxyuracil have been utilized to determine points of interaction on the DNA helix. These results establish binding by both complexes in the major groove of DNA. Differences in site recognition between enantiomers are attributed to the different hydrogen bonding and van der Waals contacts available in the major groove for the ancillary ethylenediamine ligands which differ in disposition in the two isomers.

There has been substantial interest in the rational design of small synthetic compounds which bind duplex DNA with high sequence selectivity (Pyle & Barton, 1990; Geiger-stanger et al., 1994; Sigman et al., 1993; Helene & Toulme, 1990). In particular, transition metal chemistry has been exploited for new design (Johann & Barton, 1995; Tullius, 1990; Berg, 1993; Burrows & Rokita, 1994). Our laboratory has focused on the construction of octahedral metallointercalators tailored to present an ensemble of sequence-selective contacts to the DNA major groove (Dupureur & Barton, 1995). Using a variety of methods of analysis, it is becoming apparent that metallointercalators may generally bind to DNA in the major groove. This feature may be exploited so as to construct mimics of much larger DNA-binding proteins, which similarly target DNA (Pabo & Sauer, 1992). A range of metal complexes have been prepared, taking advantage of principles of protein−nucleic acid recognition. These complexes include those which target DNA sites based upon (i) shape selection (Chow & Barton, 1992), (ii) direct readout (Krotz et al., 1993a), and (iii) sequence-dependent DNA twistability (Terbrueggen & Barton, 1995). Metallointercalators to which small peptides have been tethered also have been targeted to DNA sites with high sequence selectivity (Sardesai et al., 1994).

The characterization of DNA recognition by these small metal complexes has been substantially aided by the DNA cleavage chemistry that is associated with redox-active metal complexes (Dervan, 1986). We have recently focused on phenanthrenequinone diimine (phi) complexes of rhodium-(III) as the metallointercalators (Pyle et al., 1989; Sitlani et al., 1992; Krotz et al., 1993c). Complexes containing the $Rh(phi)^{3+}$ moiety have been shown to bind DNA avidly by intercalation. Importantly, phi complexes of rhodium(III) are also potent photooxidants, and this photochemistry may be utilized to promote DNA strand cleavage. For the complexes $Rh(phen)_2phi^{3+}$ and $Rh(phi)_2bpy^{3+}$, the products of photoinduced DNA cleavage are consistent with direct abstraction of the C3′-hydrogen atom of the deoxyribose sugar by the photoactivated, intercalated phi ligand (Sitlani et al., 1992). This DNA lesion is unique for small molecular cleaving agents in that it arises in the DNA major groove (Stubbe & Kozarich, 1987; Dedon & Goldberg, 1992). Importantly, this photoinduced DNA cleavage chemistry, involving no diffusible species, may be utilized to mark sites of binding.

Here we describe the detailed characterization of DNA recognition and photocleavage by Λ- and Δ-$Rh(en)_2phi^{3+}$. We have previously carried out studies of enantioselective recognition by octahedral metallointercalators containing bulkier ancillary ligands, where the enantiomeric differences were largely determined by matching (or not matching) the symmetry of the metal complex to that of the DNA helix (Barton, 1986; Sitlani & Barton, 1994). Here the small ethylenediamine ligands give rise to complexes that may span only two base pairs. Their simplicity lies in that they contain only two functional groups for potential interaction with the DNA duplex. As illustrated in Figure 1, upon intercalation,

† Supported by grants to J.K.B. from the National Institutes of Health (GM33309) and an NIH-NRSA predoctoral fellowship to T.P.S.

* Author to whom correspondence should be addressed.

⊗ Abstract published in *Advance ACS Abstracts,* November 1, 1995.

0006-2960/95/0434-15037$09.00/0

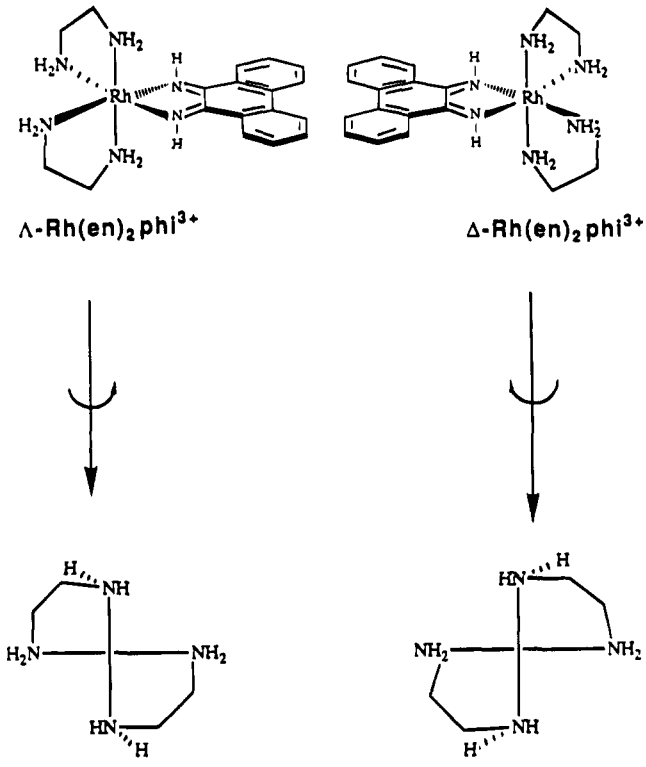

FIGURE 1: Enantiomers of Rh(en)$_2$phi^{3+}, illustrating their schematic structures (above) and the disposition of functional groups upon intercalation.

both Λ- and Δ-Rh(en)$_2$phi^{3+} contain axial and equatorial amines oriented for potential hydrogen bonding to DNA. The isomers differ with respect to the disposition of the methylene groups on the chelated ethylenediamine ligands. Hence by comparing and contrasting recognition properties of these enantiomers, it is possible to delineate specific functional group interactions (Krotz et al., 1993c). On the basis of these fundamental studies, new generations of complexes may be assembled containing an array of noncovalent interactions. Indeed, using the Rh(en)$_2$phi^{3+} unit as a starting point, the complex Δ-α-[(*R*,*R*-Me$_2$trien)Rh(phi)]$^{3+}$ has been designed and demonstrated to target the sequence 5′-TGCA-3′ using an assembly of stereochemically defined noncovalent interactions (Krotz et al., 1993a; Hudson et al., 1995).

EXPERIMENTAL PROCEDURES

Materials. Calf thymus DNA was purchased from Pharmacia LKB and plasmid pUC18 from Gibco BRL. Terminal deoxytransferase (TdT) and polynucleotide kinase (PNK) were purchased from Boehringer Mannheim. [γ-^{32}P]dATP was from Dupont-NEN, and [α-^{32}P]ddATP was from Amersham. Oligonucleotides were prepared on an ABI Model 392 DNA synthesizer using phosphoramidite chemistry and purified by reverse-phase HPLC. Reagents for solid-phase DNA oligonucleotide synthesis were purchased from ABI (Foster City, CA) and Glen Research (Sterling, VA).

The complexes [Rh(en)$_2$phi](ClO$_4$)$_3$, [Rh(NH$_3$)$_4$phi]Cl$_3$, [Rh(cyclen)phi]Cl$_3$, and [Rh(S$_4$-cyclen)phi]Cl$_3$ were prepared as previously described (Schaefer et al., 1992; Krotz et al., 1993b,c) as were Λ- and Δ-Rh(phen)$_2$phi^{3+} (Campisi et al., 1994). The resolution of Rh(en)$_2$phi^{3+} enantiomers was accomplished as follows: *rac*-[Rh(en)$_2$phi](ClO$_4$)$_3$ (32.4 mg) was preloaded onto Sephadex SP C-25 resin (5 mL) and then loaded on a 40 × 2.5 cm column. The resin was equilibrated with H$_2$O, and then the enantiomers were separated by elution with a 0.15 M solution of potassium antimonyl tartrate. Concentrations of enantiomers were quantitated by UV−visible spectroscopy (ϵ_{376nm} = 13 500 M^{-1} cm^{-1} at pH 7.0), and enantiomeric purity was assayed by CD spectroscopy ($\Delta\epsilon_{310nm}$ = ±240 M^{-1} cm^{-1}; negative value at 310 nm for the Δ-isomer) (Krotz et al., 1993b; Galbsol, 1970; Bosnich, 1969). Free base standards cytosine (C), guanine (G), thymine (T), and adenine (A) were obtained from U.S. Biochemicals and quantitated by UV−visible spectroscopy. All other enzymes, buffers, salts, and sequencing reagents were obtained from commercial sources and were of the highest purity available.

Instrumentation. UV−visible electronic spectra were recorded either on a Hewlett-Packard 8452A diode array spectrophotometer or on a Cary 2200 spectrophotometer. Circular dichroism spectra were recorded on a Jasco J500A spectrometer. The light source used in photocleavage experiments was an Oriel Model 6140 1000 W Hg/Xe lamp equipped with a Model 6123 IR filter and either a Model 77250 ($^1/_8$ m) or Model 77200 ($^1/_4$ m) monochromator. A 305 nm cutoff filter was utilized in photocleavage studies with the $^1/_8$ m monochromator to avoid DNA damage by extraneous UV light. Alternatively a 325 nm Liconix Model 4240 NB He−Cd laser was used as a light source for photocleavage. High-performance liquid chromatography (HPLC) was performed on a Waters 600E multisolvent delivery system. Phosphorimagery was performed on a Molecular Dynamics phosphorimager and processed using Image Quant software.

Photocleavage of DNA Oligonucleotides and Restriction Fragments. Oligonucleotide DNA was either 5′ end-labeled with [γ-^{32}P]ATP and polynucleotide kinase or 3′ end-labeled with [α-^{32}P]ddATP and terminal deoxytransferase using standard protocols (Maniatis & Fritsch, 1989). Labeled oligonucleotides were purified on 10% denaturing polyacrylamide gels and then isolated from gel pieces by electroelution in a Schleicher and Schuell Elutrap chamber. The conditions for examining the sequence selectivity of oligonucleotide cleavage by enantiomers of Rh(en)$_2$phi^{3+} were 100 μM base pairs of DNA (~100 000−150 000 cpm/20 μL sample), 5 μM Rh(phi)$^{3+}$ complex, pH 7.0, 10 mM sodium cacodylate, 40 mM NaCl, and irradiation for 15 min at 313 nm. Photocleavage reactions were quenched by removal from light and the addition of 1.5 μL of a 5 mM base pair calf thymus DNA solution. After irradiation, 3−5 μL (20 000−30 000 cpm) of the samples was removed, dried, and then resuspended in loading dye to a concentration of 10 000 cpm/μL of dye. Samples were heated at 90 °C for 4.5 min and then directly electrophoresed on 20% denaturing polyacrylamide gels at 2500−2800 V for 3.5 h.

The 140 and 180 base pair *Eco*RI/*Pvu*II restriction fragments of pUC18 were 3′ end-labeled with Klenow fragment and [α-^{32}P]dATP as previously described (Maniatis & Fritsch, 1989). Labeled fragments were purified by electrophoresis, excised from the gel, and isolated by electroelution. Samples were divided into 1.5 million cpm aliquots, ethanol precipitated, and stored at −20 °C. DNA stock solutions were prepared in 1.7 mL of presiliconized Eppendorf tubes which contained calf thymus DNA, 3′ end-labeled restriction fragment (~60 000−100 000 cpm/sample),

water, and buffer. Following the addition of the rhodium complex, samples were irradiated and then precipitated by the addition of 1.5 μL of a 5 mM base pair calf thymus DNA solution, 15 μL of 5 M NH_4OAc, and 400 μL of EtOH. Following precipitation, the DNA pellet was rinsed with 400 μL of 80% EtOH and then dried on a Savant rotary speed-vac. After resuspension in loading dye, samples were heated for 4.5 min at 90 °C and electrophoresed on 8% denaturing polyacrylamide gels for 2 h at 2000 V. Gels were transferred to paper and dried for 45 min using a Bio-Rad Model 583 gel dryer.

Quantitation of Cleavage Results via Phosphorimagery. Both 20% and 8% denaturing polyacrylamide gels were quantitated with a Molecular Dynamics phosphorimager. Gels were exposed to photostimulable storage phosphor screens for 12−18 h and developed using the ImageQuant program. The fraction cleavage at a base n is defined as

$$f(n) = \left(\frac{I_{n,\mathrm{raw}} - I_{\mathrm{bkgd}}}{I_{\mathrm{tot}} - I_{\mathrm{tot,bkgd}}}\right) - \left(\frac{I_{n,\mathrm{lc,raw}} - I_{\mathrm{bkgd}}}{I_{\mathrm{lc,tot}} - I_{\mathrm{lc,bkgd}}}\right) \quad (1)$$

In eq 1, $I_{n,\mathrm{raw}}$ is the integrated volume intensity of the photocleavage at base n, $I_{n,\mathrm{lc}}$ is the volume intensity for base n in the light control, and I_{bkgd} is the intensity measured for the same area placed on an ostensibly blank part of the image. Likewise, I_{tot} and $I_{\mathrm{lc,tot}}$ are the total volume intensities in either a cleavage or light control lane, including individual cleavage bands as well as uncut oligonucleotide, and $I_{\mathrm{tot,bkgd}}$ is the corresponding correction for the rectangle used to quantitate total loading in a lane. Therefore, photocleavage produced by a $Rh(phi)^{3+}$ complex is characterized by an intensity, I_n which is corrected for background and loading errors, as well as light control damage.

Determination of Affinity Constants through Photocleavage. Site affinity constants were determined by a modification of the methods developed by Singleton and Dervan (1992a,b). Photocleavage of a ^{32}P end-labeled restriction fragment was performed over a gradient of metal concentrations spanning four orders of magnitude (0.005−10 μM), and the cleavage intensities at the resolved bases in each lane were quantitated as described above. Typically, 80 bases were well resolved under the conditions used in these experiments. An average binding constant (K_b) for the $Rh(phi)^{3+}$ complex over the entire DNA fragment was determined by fitting a plot of total cleavage intensity in a lane (the numeric sum of I_n values for all resolved bases) versus total metal concentration ($[Rh]_{tot}$) to the Langmuir binding isotherm. Average affinity constants determined in this manner were wholly consistent with values predicted from UV−visible spectral titrations (data not shown). This average K_b value was then used to determine $[Rh]_{free}$ at each total rhodium concentration. Corrected cleavage intensity at an individual base ($I_{n,Rh}$) was then plotted versus $[Rh]_{free}$ and fit to a Langmuir binding isotherm to obtain individual site affinities.

Quantitation of Free Base Release. Samples were prepared in 800 μL total volume containing 50 μM $Rh(phi)^{3+}$ complex, 500 μM calf thymus DNA base pairs, 10 mM sodium cacodylate, pH 7.0, and 40 mM NaCl, in a 1.0 cm quartz UV−visible cell equipped with a small Teflon stir bar. The cell was placed in the beam of the Hg−Xe lamp such that the focal point of the lamp was in the center of the cell. To avoid bleaching a particular sample volume, cells were stirred vigorously during irradiation and also were shifted vertically three times. After irradiation, samples were divided into several Eppendorf tubes and frozen on dry ice for later HPLC analysis. Samples were injected onto a reverse-phase C18 HPLC (Microsorb-MV, Rainin Instruments, C18, 5 mM × 20 cm length, 100 Å pore size, Model 86-200-C5) column, and free base products were eluted with 0.05 M ammonium formate, pH 7.0 at 260 nm. Uncut DNA and $Rh(phi)^{3+}$ complex were removed using an acetonitrile gradient. Calibration curves for C, G, and T were constructed in order to calculate the moles free base produced in each reaction. The identity of the free base products was confirmed by coinjection with authentic standards. The photon flux of the Hg−Xe lamp was measured through ferrioxalate actinometry (Calvert & Pitts, 1967). All quantum yield determinations represent the average of two trials which differed by <5−10%.

Quantitation of Stoichiometry of Photoreaction. To determine the extent of photoaquation in the presence of DNA, samples were prepared in 1.7 mL Eppendorf tubes with 250 μL total volume containing 20 μM $Rh(en)_2phi^{3+}$ and 25 μM DNA duplex and buffered with 10 mM sodium cacodylate and 40 mM NaCl, pH 7.0. Samples were irradiated at 4 °C for 10−40 min at 313 nm. The UV−visible spectrum of each sample was measured, after which the sample was removed from the cell and frozen for later HPLC analysis. To determine the extent of free bases released, the sample was then injected onto a C18 reverse-phase column for analysis of free base products. Free bases were eluted and quantitated as described above. Then, to quantitate oligonucleotide strand cleavage, samples were prepared in 1.7 mL Eppendorf tubes with 250 μL total volume containing 20 μM $Rh(en)_2phi^{3+}$, ~500 000 cpm 3′-labeled $d(GAGTGCACTC)_2$, 25 μM DNA duplex, pH 7.0, 10 mM sodium cacodylate, and 40 mM NaCl and irradiated at 4 °C for 40 min at 313 nm. An 8 μL aliquot from each sample (~25 000 cpm) was removed, dried, and then resuspended in 3.5 μL of denaturing loading dye. Samples were heated at 90 °C for 4 min and then loaded onto 20% denaturing polyacrylamide gels. Samples were electrophoresed at 2500 V for 2 h and then quantitated by phosphorimagery.

Oligonucleotides Designed To Examine Recognition. In order to explore site-specific recognition by the metal complexes, two oligonucleotide duplexes were synthesized: Y_1, 5′-ATATC GCACG GATTA GCGTG CCTAA TC-GATAT-3′, with its complement, Y_2; and B_1, 5′-ATGCA ATATA AGTGC ACATG CAACT GCAGT GCAC-3′, with its complement, B_2.

RESULTS

Product Analysis in DNA Photocleavage by Λ- and Δ-$Rh(en)_2phi^{3+}$: DNA Termini. $Rh(en)_2phi^{3+}$ promotes DNA cleavage upon photoactivation with UV light (Krotz et al., 1993c). To examine the DNA termini produced in these photocleavage experiments, 3′-^{32}P or 5′-^{32}P end-labeled $d(GAGTGCACTC)_2$ (10 μM DNA duplex) was irradiated in the presence of 10 μM $Rh(en)_2phi^{3+}$ at 313 nm. In both 3′ and 5′ end-labeled experiments, the termini produced by Λ- and Δ-$Rh(en)_2phi^{3+}$ photocleavage were then compared to termini produced by Λ- and Δ-$Rh(phen)_2phi^{3+}$ (Sitlani et al., 1992; Campisi et al., 1994). As evident in Figure 2,

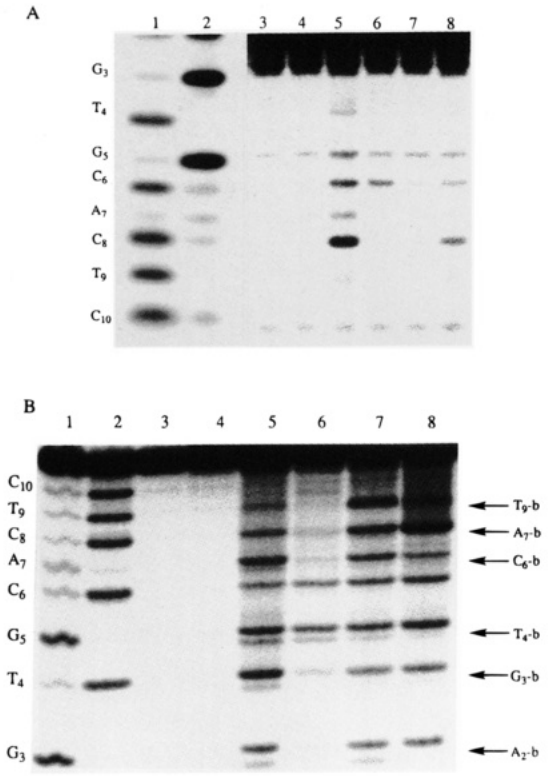

FIGURE 2: Analysis of DNA end products derived from Rh(en)$_2$phi^{3+} photocleavage. (A) Cleavage of 3′- ^{32}P end-labeled d(GAGTGCACTC)$_2$. Lanes: 1 and 2, Maxam−Gilbert C+T and G reactions, respectively; 3, DNA incubated in the presence of 5 μM Δ-Rh(en)$_2$phi^{3+}; 4, DNA irradiated in the absence of the Rh(phi)$^{3+}$ complex; 5 and 6, photocleavage for 15 min by 10 μM Λ- and Δ- Rh(en)$_2$phi^{3+}, respectively; 7 and 8, photocleavage for 10 min by 5 μM Λ- and Δ- Rh(phen)$_2$phi^{3+}, respectively. All four Rh(phi)$^{3+}$ complexes produce solely 5′-phosphate termini, as judged by comigration of photocleavage bands with those produced by Maxam−Gilbert sequencing reactions. (B) Photocleavage of 5′-^{32}P end-labeled d(GAGTGCACTC)$_2$. Lanes: 1 and 2, Maxam−Gilbert G and C+T reactions, respectively; 3−8, identical to those described for panel A. All four Rh(phi)$^{3+}$ complexes produce primarily 3′-phosphate termini, as judged by comigration with Maxam−Gilbert sequencing reactions. However, there is also clear production of a secondary photocleavage product assigned as the 3′-phosphoglycaldehyde at numerous sites (denoted with the letter b).

photocleavage of 3′-^{32}P end-labeled d(GAGTGCACTC)$_2$ by the enantiomers of both Rh(en)$_2$phi^{3+} and Rh(phen)$_2$phi^{3+} produces only 5′-phosphate terminal products; these fragments comigrate with fragments produced in Maxam−Gilbert sequencing reactions (Maniatis & Fritsch, 1989). For a range of DNA lesions, these 5′-phosphate termini would be expected (Stubbe & Kozarich, 1987). To examine the 3′-terminal lesion, Figure 2B directly compares photocleavage of 5′-^{32}P end-labeled d(GAGTGCACTC)$_2$ by Λ-and Δ-Rh(en)$_2$phi^{3+} to cleavage by Λ- and Δ-Rh(phen)$_2$phi^{3+}. On this terminus, both Λ- and Δ-Rh(en)$_2$phi^{3+} produce primarily 3′-phosphate products which comigrate with the fragments produced in the Maxam−Gilbert sequencing reactions (Maniatis & Fritsch, 1989). In addition, at several sites a secondary band is also evident, denoted with the letter b, which migrates significantly slower than the corresponding primary fragment containing a 3′-phosphate. For Λ-Rh(en)$_2$phi^{3+}, formation of this secondary product is evident at positions G$_3$, T$_4$, C$_6$, and T$_9$, while the Δ-enantiomer produces secondary bands at T$_4$, C$_6$, and T$_9$. At higher exposures, there is also a secondary band accompanying the weak cleavage by Δ-Rh(en)$_2$phi^{3+} at G$_3$. Importantly, both Λ-Rh(phen)$_2$phi^{3+} and Δ-Rh(phen)$_2$phi^{3+} also produce this secondary band at positions G$_3$, T$_4$, C$_6$, and A$_7$ in photocleavage of d(GAGTGCACTC)$_2$. This terminus has been assigned as the 3′-phosphoglycaldehyde produced in photocleavage of DNA by Rh(phen)$_2$phi^{3+} (Sitlani et al., 1992). This phosphoglycaldehyde product represents the only nonphosphate terminus observed under these conditions; in particular no phosphoglycolate product is apparent.

Quantitation indicates that the secondary phosphoglycaldehyde band accounts for ~30−50% of the cleavage by Λ-Rh(en)$_2$phi^{3+}, a higher percentage than is produced by either Λ- or Δ-Rh(phen)$_2$phi^{3+}. It is noteworthy that while the strong cleavage by the Δ-Rh(en)$_2$phi^{3+} complex at position G$_5$ is accompanied by no phosphoglycaldehyde product, cleavage at position C$_6$ produces significant amounts of phosphoglycaldehyde product. Also, the weaker cleavage by the Δ-enantiomer at T$_4$ and G$_3$ produces secondary bands which account for ~50% of the total cleavage at these weak sites. A similar high percentage of 3′-phosphoglycaldehyde has been observed at weaker cleavage sites of Λ-Rh(phen)$_2$phi^{3+} (Campisi et al., 1994).

Free Base Release. HPLC analysis of the photocleavage products of calf thymus DNA in the presence of *rac*-Rh(en)$_2$phi^{3+}, as well as with the related metallointercalators Rh(NH$_3$)$_4$phi^{3+}, Rh(cyclen)phi^{3+}, and Rh(S$_4$-cyclen)phi^{3+}, revealed the release of the free base products cytosine, guanine, and thymine (C, G, and T). The free base adenine (A) was also observed at longer retention times, but the peak was always quite broad and thus not suitable for quantitation. The yields of base products determined therefore represent underestimates. Other nucleic acid base products were not detected. In particular, base propenoic acids could not be isolated, but this absence may be a result of their photoinstability and the long irradiation times required for these experiments (Sitlani et al., 1992).

The quantum yields for free base release by *rac*-Rh(en)$_2$phi^{3+}, Rh(NH$_3$)$_4$phi^{3+}, Rh(cyclen)phi^{3+}, and Rh(S$_4$-cyclen)phi^{3+} are 1.0×10^{-4}, 0.6×10^{-4}, 1.2×10^{-4}, and 0.3×10^{-4} respectively. These values may be compared to the value of 12×10^{-4} previously reported for the quantum yield of free base release by Rh(phen)$_2$phi^{3+} (Sitlani et al., 1992). In general, the quantum yields for photoreaction of Rh(phi)$^{3+}$ complexes containing saturated amines as ancillary ligands are an order of magnitude less than the quantum yield for Rh(phen)$_2$phi^{3+}.

Stoichiometry of DNA Photoreaction with Rh(en)$_2$phi^{3+}. The photolysis of Rh(phi)$^{3+}$ complexes from 313 to 365 nm results in the preferential loss of the phi ligand, which may be monitored by the absorbance loss in the phi-centered $\pi \rightarrow \pi^*$ transition of the UV−visible spectrum. It is instructive to compare the yield for this photoaquation in the presence of DNA directly to the photocleavage of DNA. Under conditions where the photolysis of the bound complex results in a ~12% (0.60 nmol) loss of Rh(en)$_2$phi^{3+}, determined spectroscopically, we measure the production of 0.48 nmol of free bases (C, G, and T); estimation of the yield so as to include A would lead to a value of 0.6.

There is, therefore, a direct stoichiometric relationship between photoaquation and free base release. In order to relate the amount of DNA strand cleavage with the amount of photolysis and free base release, photocleavage of 3′-^{32}P

Table 1: Stoichiometry in Photocleavage of d(GAGTGCACTC) by $Rh(en)_2phi^{3+}$

experiment[a]	product (nmol)
photoaquation	0.60[b,e]
free C, G, and T released	0.48[c,e]
strand cleavage	0.58[d,f]

[a] Conditions used are given in Experimental Procedures. [b] Quantitated at 402 nm, where ϵ_{free} and ϵ_{bound} for $Rh(en)_2phi^{3+}$ are identical. [c] Determined by integration of the peaks for C, G, and T and comparison to calibration curves constructed with authentic samples. Estimation to include A yields a value of 0.6 nmol. [d] Calculated as (percentage cleaved) × (DNA strand concentration) × (250 μL) × (1.25). [e] The average of three trials. [f] The average of four trials.

end-labeled $d(GAGTGCACTC)_2$ was performed under the same conditions as described above for unlabeled samples. The cleavage reactions were analyzed by 20% denaturing polyacrylamide gel electrophoresis, and the cleavage was quantitated by phosphorimagery. On this basis 0.58 nmol DNA strands was cleaved. Therefore, under identical irradiation conditions we observe a loss of 0.60 nmol of $Rh(en)_2phi^{3+}$, production of 0.48 nmol of free C, G, and T, and cleavage of 0.58 nmol of DNA strands (Table 1). These results indicate that a 1:1:1 stoichiometry exists between the loss of phi absorbance, the release of free nucleic acid bases, and the scission of the DNA strand. It therefore appears that every $Rh(en)_2phi^{3+}$ complex which undergoes photoaquation yields productive cleavage of the DNA strand. A similarly high efficiency of reaction per activated complex was seen with $Rh(phen)_2phi^{3+}$ (Sitlani et al., 1992), although for $Rh(phen)_2phi^{3+}$ the absolute quantum yields are higher (Krotz et al., 1993b).

Site-Specific Affinity Constants from Photocleavage Experiments. Figure 3 displays cleavage of a 3′-^{32}P 140 base pair end-labeled restriction fragment by Λ- and Δ-$Rh(en)_2phi^{3+}$ over 4 orders of magnitude concentration. These data may be utilized to extract site affinity constants using quantitative affinity cleavage (Brenowitz et al., 1986a, 1986b; Senear et al., 1986; Singleton & Dervan, 1992a,b). The sequence selectivity of both complexes matches the selectivities observed in cleavage of both restriction fragments (Krotz et al., 1993c) and oligonucleotide substrates (*vide infra*). Δ-$Rh(en)_2phi^{3+}$ recognizes 5′-GC-3′ sites, while

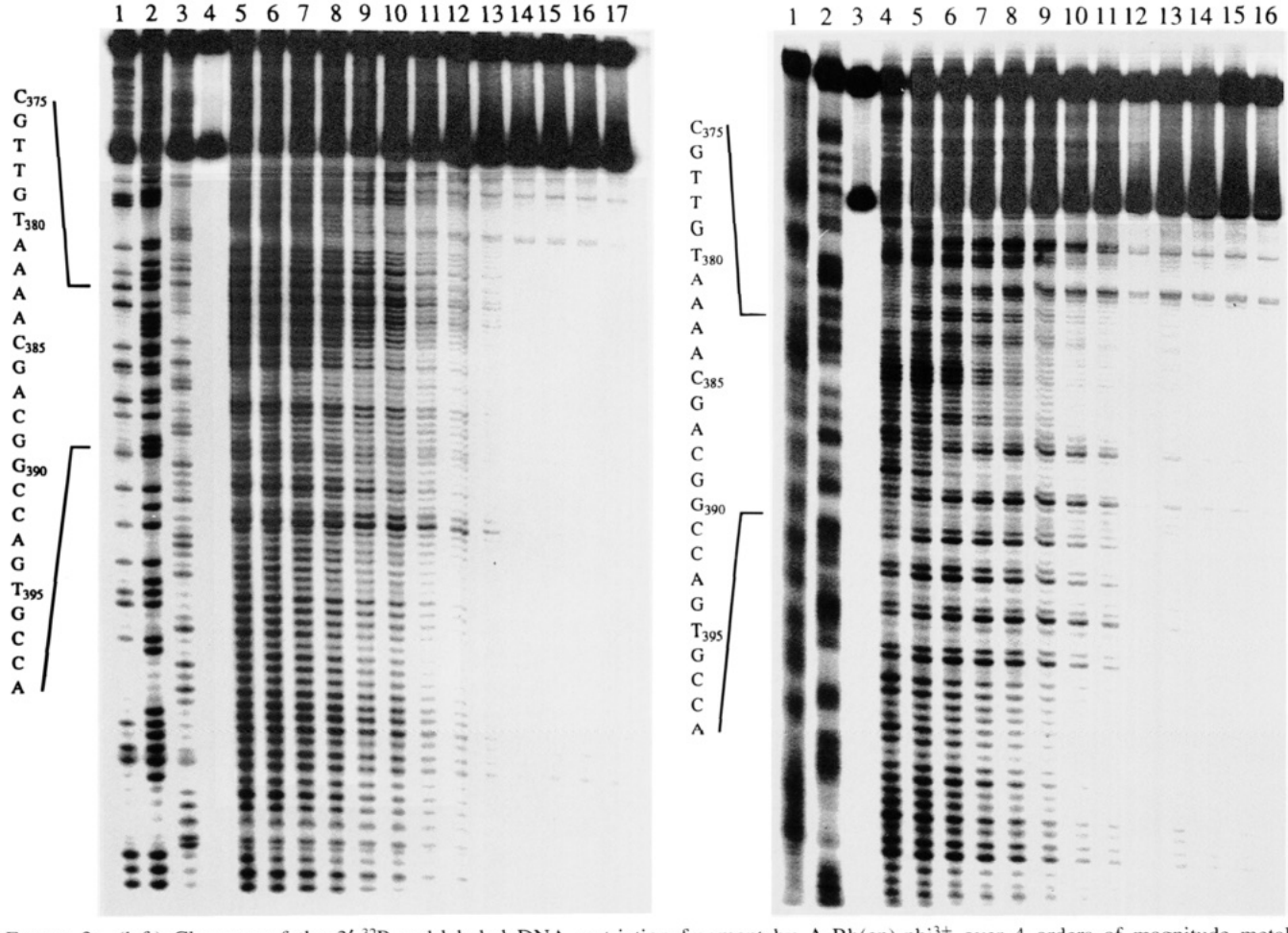

FIGURE 3: (left) Cleavage of the 3′-^{32}P end-labeled DNA restriction fragment by Λ-$Rh(en)_2phi^{3+}$ over 4 orders of magnitude metal concentration. Irradiation conditions were 10 μM calf thymus DNA base pairs, 10 mM sodium cacodylate, 40 mM NaCl, pH 7.0, and 10 min irradiation at 313 nm. Lanes: 1−3, Maxam−Gilbert G, G+A, and C+T sequencing reactions, respectively; 4, incubation of DNA with Λ-$Rh(en)_2phi^{3+}$, no irradiation; 5−16, cleavage at 10, 5, 3, 2, 1.5, 1, 0.5, 0.25, 0.1, 0.05, 0.01, and 0.005 μM metal complex; 17, irradiation of DNA in the absence of the metal complex. Note that there is saturation of numerous cleavage sites by the 0.5 μM level of metal concentration. In parallel with its sequence selectivity on oligonucleotide substrates, Λ-$Rh(en)_2phi^{3+}$ exhibits little sequence specificity on a restriction fragment substrate. (right) Cleavage of the 3′-^{32}P end-labeled DNA restriction fragment by Δ-$Rh(en)_2phi^{3+}$ over 4 orders of magnitude metal concentration. Irradiation conditions were 10 μM calf thymus DNA base pairs, 10 mM sodium cacodylate, 40 mM NaCl, pH 7.0, and 10 min irradiation at 313 nm. Lanes: 1 and 2, Maxam−Gilbert A+G and C+T sequencing reactions, respectively; 3, incubation of DNA with Δ-$Rh(en)_2phi^{3+}$, no irradiation; 16, irradiation of DNA in the absence of the metal complex; 4−15, cleavage at 10, 5, 3, 2, 1.5, 1, 0.5, 0.25, 0.1, 0.05, 0.01, and 0.005 μM metal complex.

Table 2: Site-Specific K_b Values of Λ- and Δ-Rh(en)$_2$phi^{3+} for Selected Sites of the 140 Base Pair Restriction Fragment[a]

base	Λ-Rh(en)$_2$phi^{3+} $K_{b,n}$ ($\times 10^{-6}$ M^{-1})[b]	Δ-Rh(en)$_2$phi^{3+} $K_{b,n}$ ($\times 10^{-6}$ M^{-1})[b]
C_{375}	3.3	1.0
G	3.2	0.8
T	3.3	1.0
T	3.2	1.2
G	3.0	1.4
T_{380}	2.8	1.6
A	3.1	1.5
A	3.1	1.2
A	2.1	1.2
A	1.8	1.1
C_{385}	1.9	1.3
G	1.6	1.5
A	1.7	1.5
C	1.7	0.5
G	1.1	0.4
G_{390}	1.7	0.8
C	2.7	5.0
C	1.9	0.8
A	1.6	0.3
G	1.7	0.3
T_{395}	1.7	0.7
G	1.8	3.3
C	2.9	7.7
C	2.2	2.0
A	1.7	0.9
average	2.3×10^6 M^{-1}	1.6×10^6 M^{-1}
high	3.3×10^6 M^{-1}	7.7×10^6 M^{-1}
low	1.1×10^6 M^{-1}	0.3×10^6 M^{-1}

[a] The bases are numbered by their position in the sequence of pUC18. $K_{b,n}$ values are listed for analysis using $[Rh]_{free}$ values as described. [b] Data are presented as the average of two independent determinations, with uncertainty of $\sim 0.5 \times 10^6$ M^{-1}.

Λ-Rh(en)$_2$phi^{3+} cleaves with little sequence selectivity. The occupancy of strong sites for both Λ- and Δ-Rh(en)$_2$phi^{3+} is well demonstrated by the saturation of cleavage at strong binding sites. However, this saturating level of cleavage is often decreased at higher metal concentrations due to both the population of weaker sites and the overcleavage of the labeled target DNA.

Table 2 displays affinity constants at different sites, $K_{b,n}$, for Λ- and Δ-Rh(en)$_2$phi^{3+} on the 3′-^{32}P end-labeled 140-mer restriction fragment, and Figure 4 displays representative binding isotherms derived from the cleavage data. These site affinity constants reflect the recognition patterns previously observed for these enantiomers (Krotz et al., 1993c) and are consistent with the overall binding strength estimated from spectrophotometric measurements. Δ- and Λ-Rh(en)$_2$phi^{3+} have equivalent DNA-binding affinities of 2×10^6 M^{-1}. However, the Λ-isomer is substantially sequence neutral (the range of site affinities varying only from 1 to 3 $\times 10^6$ M^{-1}), while Δ-Rh(en)$_2$phi^{3+} shows a higher sequence selectivity for GC sites (overall range of $0.3-8 \times 10^6$ M^{-1}). As expected on the basis of their small size and few possible noncovalent contacts besides intercalation, the enantiomers of Rh(en)$_2$phi^{3+} display a low level of sequence selectivity. However, this fact points out the strength of the photocleavage assay, since such small energetic differences can be readily detected.

Sequence Selectivity with Variations in the Metal Complex. In order to explore the basis for the site discrimination in more detail, DNA photocleavage by Λ- and Δ-Rh(en)$_2$phi^{3+} was compared to that by several other Rh(phi)$^{3+}$ complexes,

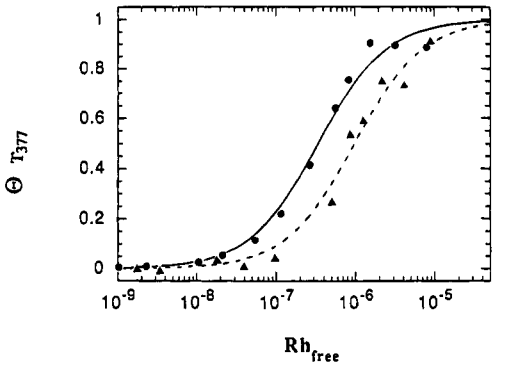

FIGURE 4: Representative binding isotherms for Λ- and Δ-Rh(en)$_2$phi^{3+}. Cleavage intensity data were quantitated as described in Experimental Procedures and fit to a Langmuir binding isotherm. Cleavage intensity was then normalized by the value of I_{sat} provided by the least squares fit and then replotted as Θ ($\Theta = I_n/I_{sat,n}$) versus $[Rh]_{free}$. Data are shown for the T_{377} base step. The triangles represent Δ-Rh(en)$_2$phi^{3+}, while the circles represent Λ-Rh(en)$_2$phi^{3+}.

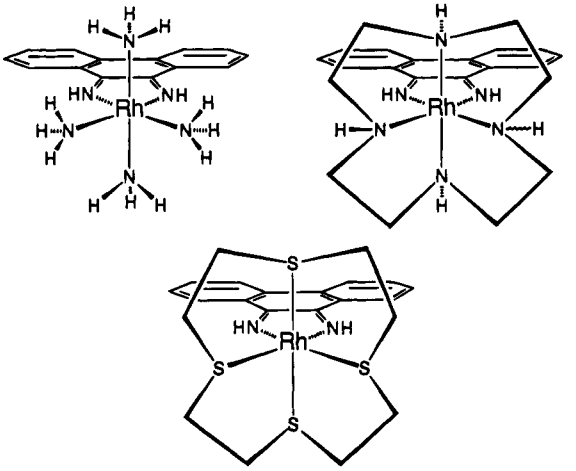

FIGURE 5: Schematic structures of the derivative Rh(phi)$^{3+}$ complexes Rh(NH$_3$)$_4$phi^{3+} (top, left), Rh(cyclen)phi^{3+} (top, right), and Rh(S$_4$-cyclen)phi^{3+} (bottom).

which differed in the type and placement of ancillary ligands (Figure 5). Comparison of the recognition patterns of these complexes offers a means to identify the structural elements in Λ- and Δ-Rh(en)$_2$phi^{3+} which may be responsible for any sequence selective recognition. For the substrate in this study, an oligonucleotide duplex ($Y_1 \cdot Y_2$) was designed to contain, on each strand, all 10 possible two-base steps. A similar comparison has been made previously on a DNA restriction fragment (Krotz et al., 1993c).

Photocleavage of the duplex $Y_1 \cdot Y_2$ by Λ- and Δ-Rh(en)$_2$phi^{3+}, as well as by Rh(NH$_3$)$_4$phi^{3+}, Rh(cyclen)phi^{3+}, and Rh(S$_4$-cyclen)phi^{3+}, is shown in Figure 6. As expected on the basis of the site affinity constants, cleavage by Δ-Rh(en)$_2$phi^{3+} is quite specific, with strong sites of cleavage concentrated at GC regions. When strand Y_2 is labeled (data not shown), strong cleavage is also found in complementary regions on the opposite strand. Recognition of $Y_1 \cdot Y_2$ by Rh(NH$_3$)$_4$phi^{3+}, which lacks the potential for making extensive van der Waals contacts with DNA, closely parallels the sequence selectivity of Δ-Rh(en)$_2$phi^{3+} (compare lanes 4 and 5 of Figure 6). In fact, there are no sites on $Y_1 \cdot Y_2$ which are cleaved by Δ-Rh(en)$_2$phi^{3+} and not also recognized by Rh(NH$_3$)$_4$phi^{3+}, indicating that axial amine ligands direct recognition of GC regions. Photocleavage by

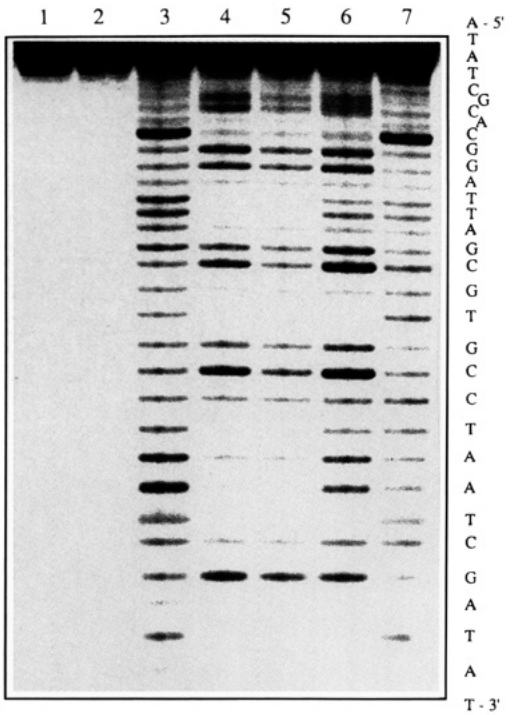

FIGURE 6: Recognition of an oligonucleotide designed to contain all 10 possible base steps: an image of a 20% denaturing polyacrylamide gel after photocleavage of oligonucleotide $Y_1 \cdot Y_2$ by Λ- and Δ-Rh(en)$_2$phi^{3+} and several derivatives. Irradiation conditions were 100 μM base pairs $Y_1 \cdot Y_2$, 3′-^{32}P end-labeled Y_1, 5 μM Rh(phi)$^{3+}$ complex, 50 mM sodium cacodylate, pH 7.0, and 20 min irradiation at 325 nm. Lanes: 1, untreated oligomer; 2, oligomer irradiated in the absence of the metal complex; 3−7, oligomer irradiated in the presence of Λ-Rh(en)$_2$phi^{3+}, Δ-Rh(en)$_2$phi^{3+}, Rh(NH$_3$)$_4$phi^{3+}, Rh(cyclen)phi^{3+}, and Rh(S$_4$-cyclen)phi^{3+}, respectively. Note that Δ-Rh(en)$_2$phi^{3+} cleaves specifically in GC-rich regions of the oligomer and that this specificity is paralleled with both Rh(NH$_3$)$_4$phi^{3+} and Rh(cyclen)phi^{3+}. Rh(S$_4$-cyclen)phi^{3+} does not cleave the duplex in GC regions but instead cleaves the oligomer shape selectively at base C$_9$ of an 5′-ACG-3′ site. Λ-Rh(en)$_2$phi^{3+} cleaves the oligomer with a low degree of site selectivity.

Rh(cyclen)phi^{3+}, which contains axial amine ligands as well as methylene groups equivalent to both Λ- and Δ-Rh(en)$_2$phi^{3+}, again shows strong cleavage in all GC regions of the duplex, in addition to weaker cleavage at bases $T_{13}T_{14}$ and $A_{24}A_{25}$ of Y_1.

In contrast to the sequence-specific cleavage of the Δ-enantiomer, Λ-Rh(en)$_2$phi^{3+} produces cleavage at nearly every residue along the duplex, consistent with its low degree of site selectivity. Thus, while Λ-Rh(en)$_2$phi^{3+} recognizes GC regions of the oligomer $Y_1 \cdot Y_2$ (e.g., $G_{20}C_{21}C_{22}$ in Figure 6), strong cleavage also occurs enantioselectively within TA stretches of the duplex. Overall within the GC regions of the $Y_1 \cdot Y_2$ duplex, enantiomeric discrimination is low, indicating that there is little energetic difference between the binding of Λ- and Δ-Rh(en)$_2$phi^{3+} at these sites. However, high levels of enantiomeric excess are observed within the TA regions of the duplex, indicating that there is an enantioselective preference of the Λ-enantiomer for TA regions of the DNA. Indeed, these results complement well the determination of site affinity constants for the two enantiomers on DNA restriction fragments (Table 2).

Importantly, the complex Rh(S$_4$-cyclen)phi^{3+}, which lacks axial amines for possible hydrogen bond donation, does not cleave the GC regions of the duplex $Y_1 \cdot Y_2$. Rh(S$_4$-cyclen)phi^{3+} cleaves the oligomer poorly, with a single strong cleavage site in Figure 6 at base C$_9$. In contrast to the generally symmetric cleavage patterns of both Λ- and Δ-Rh(en)$_2$phi^{3+}, there is no corresponding cleavage of the complementary strand when cleavage of 3′-^{32}P end-labeled Y_2 is examined (data not shown), suggesting that the binding of Rh(S$_4$-cyclen)phi^{3+} at this site may be canted asymmetrically toward one strand. Similarly, the only strong cleavage of 3′-^{32}P end-labeled Y_2 by Rh(S$_4$-cyclen)phi^{3+} again appears at a C residue of a 5′-ACG-3′ site (data not shown), and again there is no strong cleavage at the complementary site in Figure 6 (base C$_{17}$). Recognition of 5′-ACG-3′ sites by Rh(S$_4$-cyclen)phi^{3+} is ascribed to shape selectivity (Krotz et al., 1993c), since the duplex $Y_1 \cdot Y_2$ contains eight repeats of the dinucleotide 5′-CG-3′, yet only two 5′-ACG-3′ sites are recognized strongly.

Thus in cleavage of a DNA duplex of general sequence, all Rh(phi)$^{3+}$ complexes containing axial amine ligands strongly recognize GC regions of DNA, while a complex lacking hydrogen bond donors in the axial position does not cleave GC regions strongly. Furthermore, the Λ-configuration of ancillary aliphatic ligands directs the enantioselective recognition of DNA, as seen primarily in the increased affinity of Λ-Rh(en)$_2$phi^{3+} for TA regions of the duplex.

Sequence Selectivity with Variations in Nucleic Acid Bases. The sequence selectivity of Λ- and Δ-Rh(en)$_2$phi^{3+} may also be examined by introducing variations in the nucleic acid target site. The oligonucleotide duplex ($B_1 \cdot B_2$) was therefore designed to contain several 5′-GC-3′ steps, predicted to be strong sites for Δ-Rh(en)$_2$phi^{3+}, as well as a TA stretch predicted to contain strong sites for enantioselective recognition by Λ-Rh(en)$_2$phi^{3+}. Photocleavage of $B_1 \cdot B_2$ by the enantiomers of Rh(en)$_2$phi^{3+}, displayed in Figure 7, closely follows the recognition patterns established earlier. Figure 7 also includes quantitation of this cleavage in histogram format. When strand B_2 is 3′-^{32}P end-labeled, Δ-Rh(en)$_2$phi^{3+} cleaves the duplex selectively at three 5′-GC-3′ steps—$G_{14}C_{15}$, $G_{20}C_{21}$, and $G_{26}C_{27}$. At these sites, two strong cleavage bands are observed, corresponding to scission of the 5′- and the 3′-sugars of the 5′-GC-3′ intercalation step. Interestingly, this cleavage intensity at the 3′-C residue is typically twice the intensity at the 5′-G residue. This cleavage pattern is in contrast to that seen upon photocleavage of DNA by Rh(phen)$_2$phi^{3+}, which produces a single cleavage band at the 5′-base of the intercalation site (Sitlani et al., 1992).

The histogram furthermore illustrates that, for both enantiomers, strong cleavage of one strand of the duplex is accompanied by strong cleavage of the complementary strand, suggesting the absence of canting of the metal complex toward one strand within the intercalation site. Thus, the cleavage by Λ-Rh(en)$_2$phi^{3+} within TA stretches is strong on both strands, and the recognition of 5′-GC-3′ steps by Δ-Rh(en)$_2$phi^{3+} is characterized by strong cleavage at all four residues. Interestingly, these histograms reveal a distinct 3′-asymmetry in cleavage of 5′-GC-3′ steps by Δ-Rh(en)$_2$phi^{3+}, cleavage which is commonly associated with minor groove binding molecules such as MPE−Fe(II) (Sluka et al., 1987). Variations in nucleic acid base substitution (*vide infra*), however, support a major groove assignment instead. NMR studies (Shields & Barton, 1995) indicate that this cleavage pattern may emanate from the very deep intercalation by Rh(en)$_2$phi^{3+} so as to juxtapose the phi to the 3′-sugar. Overall,

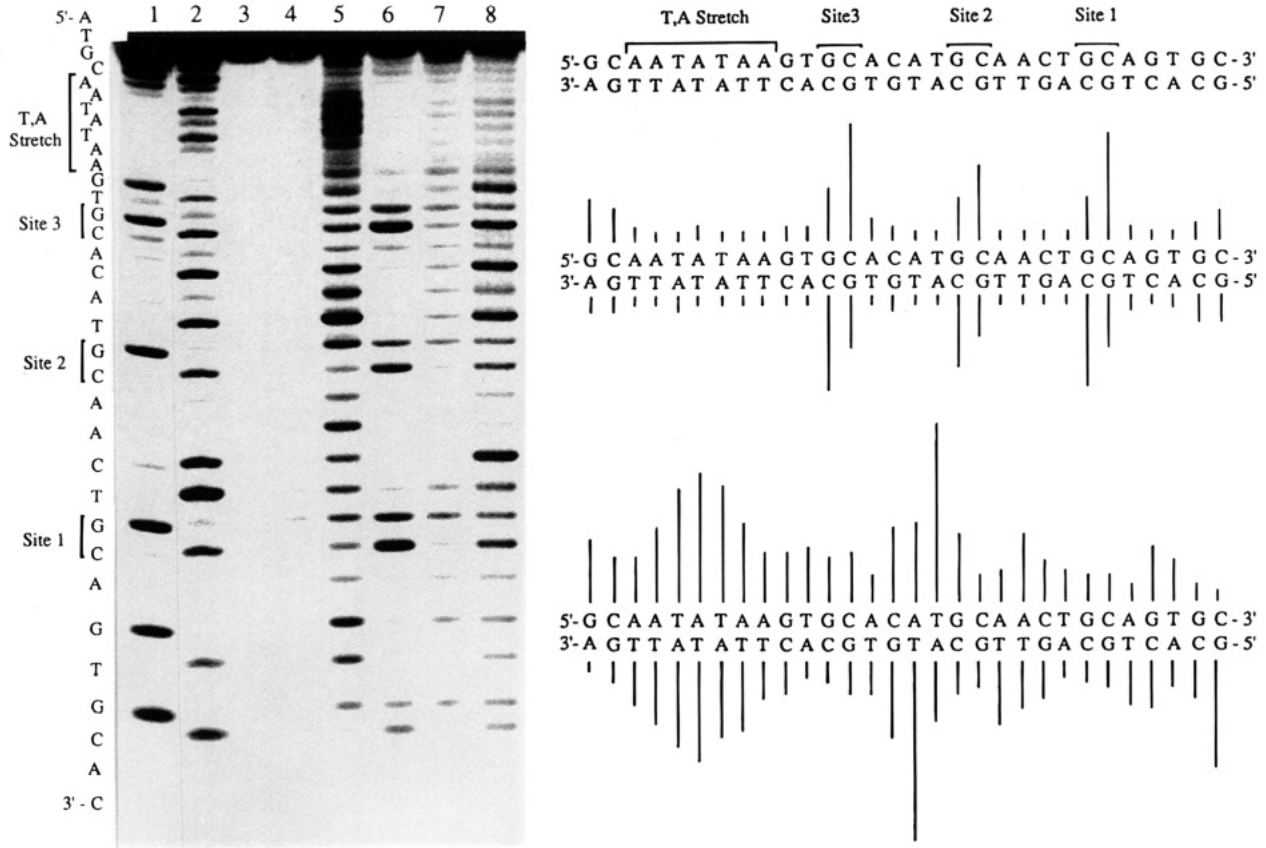

FIGURE 7: Recognition of an oligonucleotide designed to contain strong binding sites for Λ- and Δ-Rh(en)$_2$phi^{3+}, showing an image of a phosphorimaged screen (left) of a 20% denaturing polyacrylamide gel after photocleavage of the oligonucleotide $B_1 \cdot B_2$ by the enantiomers of Rh(en)$_2$phi^{3+} and a histogram (right) quantitating photocleavage of the oligomer. The top panel on the right shows the design of the oligomer. The center and lower panels display the histograms for cleavage by Δ- and Λ- Rh(en)$_2$phi^{3+}, respectively. Irradiation conditions were 100 μM base pairs $B_1 \cdot B_2$, 3′-^{32}P end-labeled strand B_1, 5 μM Rh(en)$_2$phi^{3+}, 50 mM sodium cacodylate, pH 7.0, and 15 min irradiation at 313 nm. Lanes: 1 and 2, Maxam−Gilbert G and C+T sequencing reactions, respectively; 3, oligomer incubated in the presence of Δ-Rh(en)$_2$phi^{3+}, no irradiation; 4, oligomer irradiated in the absence of the metal complex; 5 −8, oligomer irradiated in the presence of Λ-Rh(en)$_2$phi^{3+}, Δ-Rh(en)$_2$phi^{3+}, Λ-Rh(phen)$_2$phi^{3+}, and Δ-Rh(phen)$_2$phi^{3+}, respectively.

the recognition characteristics for each enantiomer are consistent with the site affinities already described.

Cleavage of Oligonucleotides Containing O^6-Methylguanine, 7-Deazaguanine, and Deoxyuracil Bases. Modifications of nucleic acid bases were also introduced to probe specific contacts of the metal complex in the DNA major groove. Although base modifications can locally perturb the DNA structure, the modifications made here are quite conservative, and direct comparisons are provided to sites lacking the modification. Indeed, it is evident in these studies that cleavage above and below the sites of modification is unperturbed, an indication that the recognition itself is remarkably localized.

To examine hydrogen-bonding contacts with the guanine O6 position, the oligonucleotide $B_1 \cdot B_2$ was modified by substitution of O^6-methylguanine residues for guanine at one of three 5′-GC-3′ steps along the duplex. Cleavage of this modified duplex is displayed in Figure 8, for the case where both guanine residues of site 3 are modified and the 3′-^{32}P label is placed on the modified B_2 strand. While Δ-Rh(en)$_2$phi^{3+} strongly cleaves the two unmodified 5′-GC-3′ steps (sites 1 and 2 in Figure 8), there is little recognition at the modified 5′-GC-3′ step (site 3). Cleavage by Λ-Rh(en)$_2$phi^{3+} at the modified 5′-GC-3′ site also is decreased relative to cleavage of unmodified site 3, although the overall cleavage by Λ-Rh(en)$_2$phi^{3+} at this site is weak on both oligomers. Quantitation of intensities indicates that the substitution of the O^6-methylguanine residues consistently decreases recognition of site 1 by a factor of 3−4-fold. Importantly, this result supports binding by the complex in the DNA major groove.

Because the steric bulk of the methyl substituent may perturb potential hydrogen bonding to the guanine N7 atom and thereby inhibit cleavage, we also synthesized a derivative of the $B_1 \cdot B_2$ duplex containing a 5′-GC-3′ step substituted with either a single 7-deazaguanine or a single O^6-methylguanine. In Figure 9, photocleavage of the mixed duplex $N^7B_1 \cdot B_2$ by Λ- and Δ-Rh(en)$_2$phi^{3+} is compared to cleavage of the similarly constructed mixed duplex $meB_1 \cdot B_2$. The results reveal that Δ-Rh(en)$_2$phi^{3+} is able to recognize a 5′-GC-3′ step containing a deazaguanine residue, while cleavage intensity at the same step is lost when a single O^6-methylguanine residue is placed on the complementary strand. The cleavage of site 3 substituted with 7-deazaguanine is similar to the cleavage of sites 1 and 2 in Figure 9, as well as to the cleavage of site 3 in the unmodified duplex. The result obtained with deazaguanine substitutions therefore neatly complements the results of O^6-methylguanine substitutions, and together they present a strong argument that the recognition of 5′-GC-3′ steps by Δ-Rh(en)$_2$phi^{3+} involves a hydrogen bond from the axial amines to the O6 position of guanine residues above and below the plane of intercalation.

In addition to probing hydrogen-bonding contacts with O^6-methylguanine and 7-deazaguanine substitutions, we also

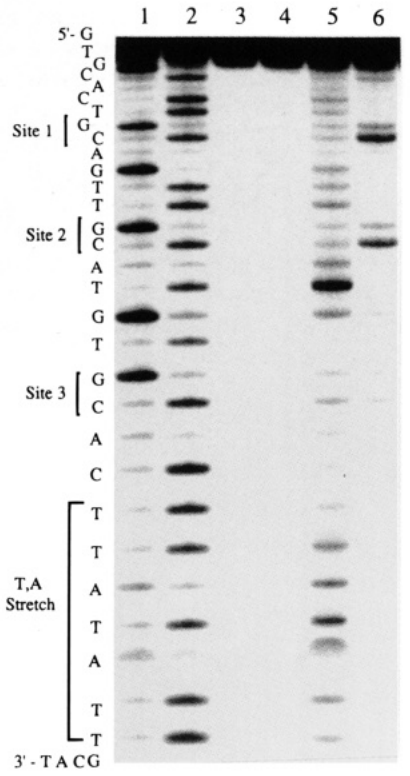

FIGURE 8: Photocleavage of an oligonucleotide duplex containing an O^6-methylguanine residue at the 5′-GC-3′ step: an image of a phosphorimaged screen of a 20% denaturing polyacrylamide gel after photocleavage by Λ- and Δ-Rh(en)$_2$phi^{3+} of a derivative of oligonucleotide B_1•B_2, where O^6-methylguanine has been substituted for both guanine residues at the 5′-GC-3′ step (site 3). Irradiation conditions were 100 μM base pairs of DNA, 3′-^{32}P end-labeled strand meB_2, 5 μM Rh(en)$_2$phi^{3+}, 10 mM sodium cacodylate, 40 mM NaCl, pH 7.0, and 15 min irradiation at 313 nm. Lanes: 1 and 2, Maxam−Gilbert G and C+T sequencing reactions, respectively; 3, oligomer incubated with Δ-Rh(en)$_2$phi^{3+}, no irradiation; 4, oligomer irradiated in the absence of the metal complex; 5 and 6, oligomer irradiated in the presence of Λ-Rh(en)$_2$phi^{3+} and Δ-Rh(en)$_2$phi^{3+}, respectively. Note that Δ-Rh(en)$_2$phi^{3+} cleaves strongly at the two unmodified 5′-GC-3′ steps of the oligomer but weakly at the third site where O^6-methylguanine has been substituted for guanine residues (site 3). Λ-Rh(en)$_2$phi^{3+} cleavage at the modified site is also slightly lower than cleavage of the similar site in the unmodified oligonucleotide.

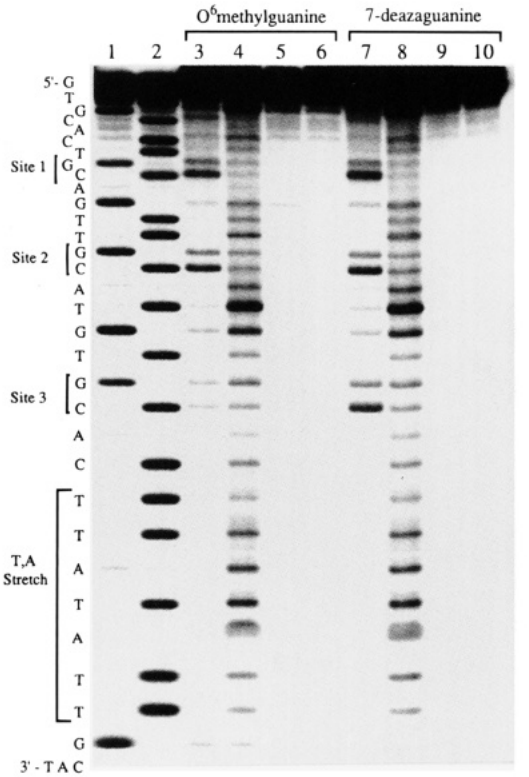

FIGURE 9: Photocleavage of an oligonucleotide containing a 5′-GC-3′ step substituted with a single O^6-methylguanine or 7-deazaguanine residue: an image of a phosphorimaged screen of a 20% denaturing polyacrylamide gel after photocleavage of the mixed duplex oligonucleotides meB_1•B_2 and N^7B_1•B2 by Λ- and Δ-Rh(en)$_2$phi^{3+}. Irradiation conditions were 100 μM base pairs of duplex, 3′-^{32}P end-labeled strand B_2, 5 μM Rh(en)$_2$phi^{3+}, 10 mM sodium cacodylate, 40 mM NaCl, pH 7.0, and 15 min irradiation at 313 nm. Lanes: 1 and 2, Maxam−Gilbert C+T and G sequencing reactions, respectively; 3 and 7, oligomer irradiated in the presence of Δ-Rh(en)$_2$phi^{3+}; 4 and 8, oligomer irradiated in the presence of Λ-Rh(en)$_2$phi^{3+}; 5 and 9, oligomer irradiated in the absence of the metal complex; 6 and 10, oligomer in the presence of Δ-Rh(en)$_2$phi^{3+}, no irradiation. Note that Δ-Rh(en)$_2$phi^{3+} cleaves strongly at the two unmodified 5′-GC-3′ sites of both duplexes but weakly at the third site where O^6-methylguanine has been substituted for the guanine residues. However, when 7-deazaguanine is placed at this 5′-GC-3′ site, strong cleavage is again observed, similar to that observed at the two unmodified sites. This result indicates that hydrogen bond donation by the axial amines of Rh(en)$_2$phi^{3+} is directed to the O^6 position of guanine, not the N^7 position.

have probed possible van der Waals contacts with the thymine methyl moiety in the enantioselective recognition of 5′-TA-3′ steps (Krotz et al., 1993c). The preference of Λ-Rh(en)$_2$phi^{3+} for 5′-TX-3′ steps suggested the importance of van der Waals contacts between the methylene groups of the ethylenediamine ligands and the thymine methyl group, located in the major groove. The disposition of methylene groups for the Λ-enantiomer permits such contact; the Δ-enantiomer does not.

To demonstrate the involvement of specific methyl−methylene interactions in enantioselective photocleavage by Λ-Rh(en)$_2$phi^{3+}, two 5′-TA-3′ sites within the oligomer Y_1•Y_2 were substituted with deoxyuracil at both thymine residues. Figure 10 shows photocleavage by Λ- and Δ-Rh(en)$_2$phi^{3+} of both the modified and unmodified duplexes. Importantly, removal of the methyl group from the major groove of DNA served to eliminate enantioselective cleavage at one 5′-UA-3′ step and reduce it at another. The smaller decrease in enantioselectivity at the 3′-A residues of both 5-TA-3′ steps indicates that, as with cleavage of 5′-GC-3′ sites by Δ-Rh(en)$_2$phi^{3+}, there is access to both sugar residues by Λ-Rh(en)$_2$phi^{3+} at a 5′-TA-3′ step. Moreover, little effect is seen in photocleavage of other 5′-TX-3′ steps, providing a useful internal standard for the modification of the thymine residues.

DISCUSSION

DNA Photocleavage by Rh(en)$_2$phi^{3+}. The product analysis associated with the photocleavage of DNA by Rh(en)$_2$phi^{3+} is consistent with a route analogous to that described for Rh(phen)$_2$phi^{3+} (Sitlani et al., 1992). The observation of the release of free nucleic acid bases in photocleavage of DNA by Rh(en)$_2$phi^{3+} and its derivatives first establishes that, as with Rh(phen)$_2$phi^{3+}, the target for photoactivated damage of DNA is the deoxyribose sugar moiety. The production of 5′-phosphate termini is common to several DNA lesions and thus does not serve to discriminate among the initial sites of reaction on the sugar. However, photocleavage of 5′-^{32}P end-labeled oligonucleotides by the enantiomers of Rh(en)$_2$phi^{3+} yields not only

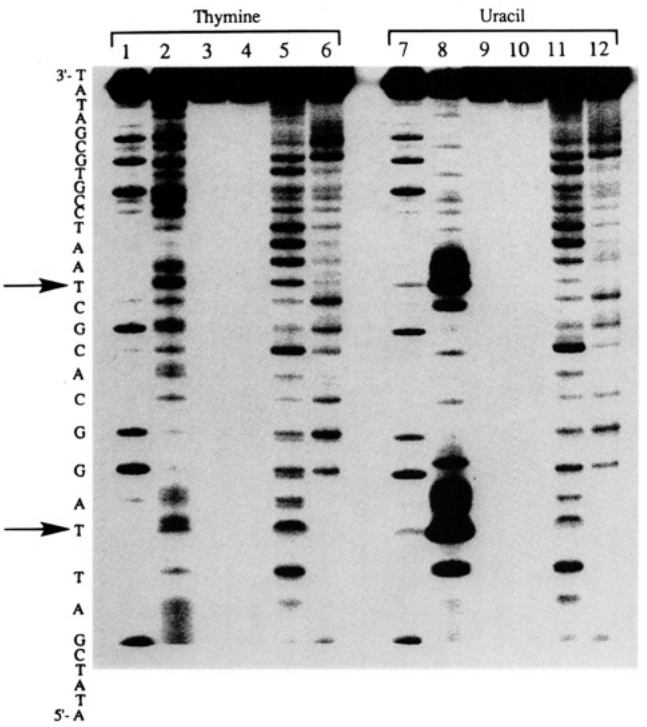

FIGURE 10: Photocleavage of oligonucleotides containing 5′-TA-3′ and 5′-UA-3′ steps: an image of a phosphorimaged screen of a 20% denaturing polyacrylamide gel after irradiation of the oligonucleotides $Y_1{\cdot}Y_2$ and $Y_1U{\cdot}Y_2U$ in the presence of Λ- and Δ-Rh(en)$_2$phi^{3+}. Irradiation conditions were 100 μM base pairs of DNA, 3′-^{32}P end-labeled strand Y_2 or Y_2U, 5 μM Rh(en)$_2$phi^{3+}, 10 mM sodium cacodylate, 40 mM NaCl, pH 7.0, and 15 min irradiation at 313 nm. Lanes 1−6 display cleavage of the 3′-^{32}P end-labeled Y_2; lanes 7−12 display cleavage of 3′-^{32}P end-labeled Y_2U. Lanes: 1 and 7, Maxam−Gilbert G reactions; 2 and 8, Maxam−Gilbert C+T reactions; 3 and 9, untreated DNA; 4 and 10, oligomer irradiated in the absence of the metal complex; 5 and 11, oligomer irradiated in the presence of Λ-Rh(en)$_2$phi^{3+}; 6 and 12, oligomer irradiated in the presence of Δ-Rh(en)$_2$phi^{3+}. Enantioselective cleavage is constant from one oligomer to the other, except at 5′-TA-3′ steps where deoxyuracil substitutions have been made. Here it appears that enantioselectivity either decreases (T_9A_{10}) or is eliminated ($T_{18}A_{19}$), indicating that the enantioselective recognition of these 5′-TA-3′ steps by Λ-Rh(en)$_2$phi^{3+} depends upon positive van der Waals contacts made with the methyl group of thymine residues, which are located in the major groove.

3′-phosphate termini, as does Rh(phen)$_2$phi^{3+}, but also the same secondary product assigned as the 3′-phosphoglycaldehyde terminus. This terminus is expected following C3′-H abstraction with subsequent degradation of the deoxyribose sugar along an O_2-dependent pathway (Sitlani et al., 1992; Stubbe & Kozarich, 1987). The greater production of the 3′-phosphoglycaldehyde terminus as a percentage of total cleavage by Rh(en)$_2$phi^{3+} compared to Rh(phen)$_2$phi^{3+} may be attributed to an increased accessibility of O_2 to the initial lesion afforded by the smaller size of Rh(en)$_2$phi^{3+}. A similar relationship was noted in the comparison of Rh(phen)$_2$phi^{3+} and Rh(phi)$_2$bpy^{3+}, where the greater production of 3′-phosphoglycaldehyde termini by Rh(phi)$_2$bpy^{3+} correlated well with the way in which the shapes of these complexes controlled access of O_2 to the initial C3′ lesion (Sitlani et al., 1992; Campisi et al., 1994). The detection of the same product upon photocleavage with enantiomers of Rh(en)$_2$phi^{3+} versus Rh(phen)$_2$phi^{3+} indicates that the cleavage mechanism established for Rh(phen)$_2$phi^{3+} may also arise with phi complexes of rhodium containing aliphatic amines.

The stoichiometry of the photocleavage reaction was also determined by comparing the amounts of Rh(en)$_2$phi^{3+} photolysis, free base release, and DNA strand cleavage under identical conditions, and these data reinforce the parallel to the reactions of Rh(phen)$_2$phi^{3+}. The stoichiometric relationship between the release of free base, strand scission, and loss of phi absorbance indicates that once activated, productive photocleavage by DNA-bound Rh(en)$_2$phi^{3+}, with free base release, occurs; the primary route for photocleavage is that which has been characterized. The lower photoefficiency of Rh(en)$_2$phi^{3+} compared to Rh(phen)$_2$phi^{3+} mirrors its lower photoaquation efficiency compared to Rh(phen)$_2$phi^{3+} (Krotz et al., 1993b). However, as with Rh(phen)$_2$phi^{3+}, with the complex deeply intercalated, photoactivation leads to strand scission. A productive reaction depends upon the intimate association of the activated phi ligand with the DNA helix.

DNA Sequence Selectivity of Rh(en)$_2$phi^{3+} Enantiomers. The enantiomers of Rh(en)$_2$phi^{3+}, like other Rh(phi)$^{3+}$ complexes, bind duplex DNA with binding affinities in the range of 10^6 M^{-1}, where the sites selected for each enantiomer are determined by the ancillary ligands. While the intercalative phi ligand imparts the high-level DNA affinity, the ethylenediamine ligands tune the affinities for different sequences. In fact, only a moderate level of selectivity is observed, as expected given the small size of these complexes with respect to even a dinucleotide DNA intercalation step. By examining the recognition characteristics of several different Rh(phi)$^{3+}$ complexes and by delineating the perturbations in recognition by Rh(en)phi^{3+} enantiomers on oligonucleotides containing modified bases, we may pinpoint the elements of this site selectivity.

A crucial observation is that recognition of DNA by Rh(en)$_2$phi^{3+} occurs within the major groove. Although this conclusion was supported indirectly by the observation of DNA cleavage products consistent with reaction at the C3′-hydrogen position, it is clearly supported here by the changes in recognition observed upon the addition or removal of a single methyl group from the major groove of DNA. Recognition by Rh(en)$_2$phi^{3+} enantiomers is perturbed by methylation of the guanine O6 atom, and enantioselectivity for 5′-TX-3′ sites is perturbed by substitution of the T by dU. These studies therefore support a major groove orientation, as has a range of earlier studies on different metallointercalators (Wang et al., 1978; Rehmann & Barton, 1990a,b; David & Barton, 1993; Dupureur & Barton, 1993; Collins et al., 1994; Sitlani et al., 1993; Terbreuggen & Barton, 1995).

Models for DNA Site Recognition by Enantiomers. On the basis of the data presented, we may examine the basis for DNA site selectivity using molecular modeling. Figure 11 displays models of Λ- and Δ-Rh(en)$_2$phi^{3+} intercalated into 5′-TA-3′ and 5′-GC-3′ steps, respectively. The models were constructed using crystallographic coordinates for Rh(en)$_2$phi^{3+} (Schaefer et al., 1992) and energy-minimized intercalation sites. These qualitative models provide a useful structural context in which to consider the data obtained. As evident in both panels of Figure 11, the size of the enantiomers of Rh(en)$_2$phi^{3+} is slightly smaller than the height along the helix axis of an intercalated base pair step. Hence at best, without conformational distortion, two-base site selectivity is expected for both Λ- and Δ-Rh(en)$_2$phi^{3+}. The two-base site size of Rh(en)$_2$phi^{3+} contrasts the four-

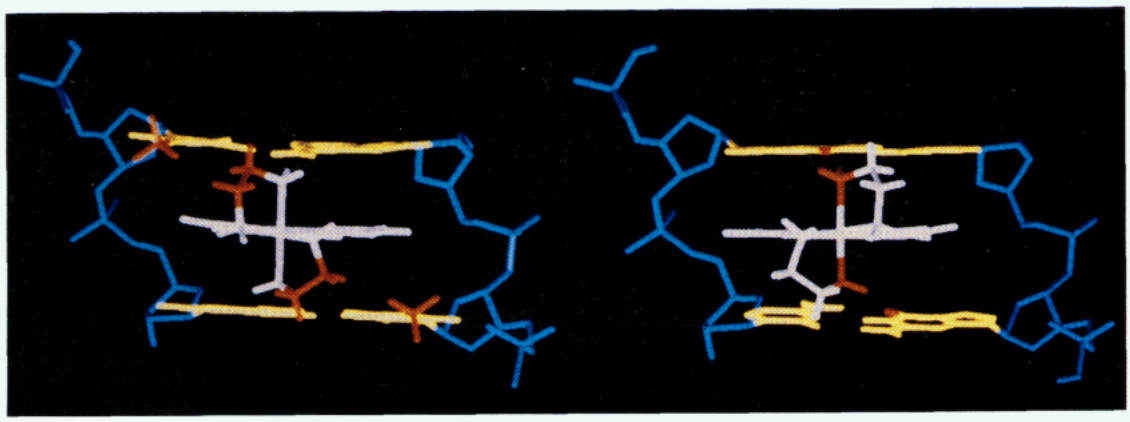

FIGURE 11: Modeling of $Rh(en)_2phi^{3+}$ enantiomers in two intercalation sites. In these models, Λ-$Rh(en)_2phi^{3+}$ is illustrated on the left in a 5′-TA-3′ step, and Δ-$Rh(en)_2phi^{3+}$ is displayed on the right intercalated into a 5′-GC-3′ step. The interactions of interest are highlighted in red. The remainder of the metal complex is shown in white, the DNA base pairs are in yellow, and the sugar−phosphate backbone is in blue. The hydrogen bonding between axial amines of the complex and the 5′-guanine residues of the 5′-GC-3′ steps is illustrated on the right. The axial amines (in red) of Δ-$Rh(en)_2phi^{3+}$ are well positioned to donate a hydrogen bond to the O6 of guanine (also in red). Identical interactions are available to the axial amines of the Λ-isomer. The methylene−methyl contacts responsible for enantioselective cleavage by Λ-$Rh(en)_2phi^{3+}$ at the 5′-TX-3′ steps are illustrated on the left. The disposition of methylene groups for Λ-$Rh(en)_2phi^{3+}$ complements well the positioning of methyl groups of thymines above and below the site of intercalation in a 5′-TA-3′ step. The methylene groups of the ethylenediamine ligands have been highlighted in red in order to show their proximity (4 Å) to the thymine methyl moieties, also in red.

base pair site size of $Rh(phen)_2phi^{3+}$ and other tris(polypyridyl) complexes, where the size of the complex is comparable to the size of the major groove, and overall enantioselectivities favoring the Δ-isomer are observed with right-handed DNA helices (Sitlani & Barton, 1994; Barton, 1986).

At the two-base level, the preferences in cleavage by Λ- and Δ-$Rh(en)_2phi^{3+}$ are readily illustrated with these models. As evident in Figure 11, the disposition of methylene groups for Λ-$Rh(en)_2phi^{3+}$ complements well the positioning of methyl groups of thymines above and below the site of intercalation. The methylene groups of the ethylenediamine ligands have been highlighted in red in order to show their proximity to the thymine methyl moieties, also in red. In this model the distances are not too close so as to provide a steric blockade for the Λ-isomer but sufficiently close to allow a stabilizing van der Waals contact. Clearly, an equivalent nonbonded contact would not be available with the Δ-isomer at the 5′-TA-3′ step. It is noteworthy that the right-handed helicity of DNA precludes a complementary interaction of the Δ-isomer at a 5′-AT-3′ step.

The appropriate positioning of the axial amines of $Rh(en)_2phi^{3+}$ for potential hydrogen bonding with the O6 position of guanine residues is illustrated also in Figure 11. Although this model describes the hydrogen-bonding interactions of Δ-$Rh(en)_2phi^{3+}$ at a 5′-GC-3′ base pair step, similar hydrogen-bonding interactions would be available for the Λ-isomer. As seen in the figure, the axial amines (in red) of Δ-$Rh(en)_2phi^{3+}$ are well poised to donate a hydrogen bond to the O6 position of guanine (also in red). N---O distances of 3.0 Å to the guanines above and below the intercalating phi may be obtained with O···H−N angles of $>160°$. It is also noteworthy that, in order to position the equatorial amines for hydrogen bonding to the phosphate backbone, substantial canting of the complex toward one strand would be required.

Thus the sequence selectivities determined experimentally are explained through models invoking hydrogen bonding and van der Waals contacts between Λ- and Δ-$Rh(en)_2phi^{3+}$ and the major groove of DNA. The 5′-GC-3′ targeting observed with both Λ- and Δ-$Rh(en)_2phi^{3+}$ may be attributed to specific hydrogen bonding by the axial amines of the complex, while the enantioselective targeting of 5′-TA-3′ steps by Λ-$Rh(en)_2phi^{3+}$ is attributed to stabilizing van der Waals interactions of the methylene groups of the ethylenediamine ligands with thymine methyl groups in the DNA major groove. Once the orientation of the metal complex is determined through intercalation, the orientation of the ancillary functionalities for potential interaction with DNA becomes well-defined and permits predictably design of sequence-selective interactions.

Implications for Design. These studies expand the range of octahedral metallointercalators to be applied in developing a family of small, synthetic metal complexes to recognize an array of DNA sequences. The phi ligand provides an appropriate high-affinity anchor through intercalation in the major groove of DNA. For different ancillary ligands, the photochemistry of the $Rh(phi)^{3+}$ moiety is preserved to mark sites of binding. The ancillary ligands may be varied, however, to read different sequences in the major groove through an ensemble of hydrogen bonding and van der Waals contacts. Variations in ligand assemblies on the octahedral $Rh(phi)^{3+}$ scaffold can be accomplished to vary sites selected, and indeed even simple variations between enantiomers affect the sequence targeted. Hence, these studies, using perhaps the simplest ancillary ligand, ethylenediamine, in two different chelated dispositions, may serve to underscore simply the sensitivity and scope of this strategy of constructing octahedral metallointercalators as predictable DNA sequence-selective agents.

REFERENCES

Barton, J. K. (1986) *Science 233*, 727.

Berg, J. M. (1993) *Curr. Opin. Struct. Biol. 3*, 11.

Bosnich, B. (1969) *Acc. Chem. Res. 2*, 266.

Brenowitz, M., Senear, D. F., Shea, M. A., & Ackers, G. K. (1986a) *Methods Enzymol. 130*, 132.

Brenowitz, M., Senear, D. F., Shea, M. A., & Ackers, G. K. (1986b) *Proc. Natl. Acad. Sci. U.S.A. 83*, 8462.

Burrows, C. J., & Rokita, S. E. (1994) *Acc. Chem. Res. 27*, 295.

Calvert, J. G., & Pitts, J. N. (1967) *Photochemistry*, John Wiley and Sons, New York.
Campisi, D., Morii, T., & Barton J. K. (1994) *Biochemistry 33*, 4130.
Chow, C. S., & Barton, J. K. (1992) *Methods Enzymol. 212*, 219.
Collins, J. G., Shields, T. P., & Barton, J. K. (1994) *J. Am. Chem Soc. 116*, 9840.
David, S. D., & Barton, J. K. (1993) *J. Am. Chem. Soc. 115*, 2984.
Dedon, P. C., & Goldberg, I. H. (1992) *Chem. Res. Toxicol. 5*, 311.
Dervan, P. B. (1986) *Science 232*, 464.
Dupureur, C. M., & Barton, J. K. (1993) *J. Am. Chem. Soc. 116*, 1086.
Dupureur, C. M., & Barton. J. K. (1995) *Compr. Supramol. Chem.* (in press).
Galbsol, F. (1970) *Inorg. Synth. 12*, 269.
Geierstanger, B. H., Mrksich, M., Dervan, P. B., & Wemmer, D. E. (1994) *Science 266*, 646.
Hélène, C., & Toulmé, J. J. (1990) *Biochim. Biophys. Acta 1049*, 99.
Hudson, B. P., Dupureur, C. M., & Barton, J. K. (1995) *J. Am. Chem. Soc.* (in press).
Johann, T. W., & Barton, J. K. (1995) *Adv. Coord. Chem., Trans. A, R. Soc.* (in press).
Krotz, A. H., Hudson, B. P., & Barton, J. K.(1993a) *J. Am. Chem Soc. 115*, 12577.
Krotz, A. H., Kuo, L. Y., & Barton, J. K. (1993b) *Inorg. Chem 32*, 5963.
Krotz, A. H., Kuo, L. Y., Shields, T. P., & Barton, J. K. (1993c) *J. Am. Chem Soc. 115*, 3877.
Maniatis, T., Fritsch, E. F., & Sambrook, J. (1989) *Molecular Cloning: A Laboratory Manual*, 2nd ed., Cold Spring Harbor Laboratory, Cold Spring Harbor, NY.
Pabo, C. O., & Sauer, R. T. (1992) *Annu. Rev. Biochem. 61*, 1053.
Pyle, A. M., & Barton, J. K. (1990) *Prog. Inorg. Chem. 38*, 413.
Pyle, A. M., Long, E. C., & Barton, J. K. (1989) *J. Am. Chem. Soc. 111*, 4520.
Rehmann, J. P., & Barton, J. K. (1990a) *Biochemistry 29*, 1701.
Rehmann, J. P., & Barton, J. K. (1990b) *Biochemistry 29*, 1710.
Sardesai, N. Y., Zimmermann, K., & Barton, J. K. (1994) *J. Am. Chem. Soc. 116*, 7502.
Schaefer, W. P., Krotz, A. H., Kuo, L. Y., Shields, T. P., & Barton, J. K. (1992) *Acta Crystallogr. C48*, 2071.
Senear, D. F., Brenowitz, M., Shea, M. A., & Ackers, G. K.(1986) *Biochemistry 25*, 7344.
Shields, T. P., & Barton, J. K., (1995) *Biochemistry 34*, 15049–15056.
Sigman, D. S., Mazumder, A., & Perrin, D. M. (1993) *Chem. Rev. 93*, 2295.
Singleton, S. F, & Dervan, P. B. (1992a) *Biochemistry 31*, 10995.
Singleton, S. F, & Dervan, P. B. (1992b) *J. Am. Chem Soc. 114*, 6957.
Sitlani, A., & Barton, J. K. (1994) *Biochemistry 33*, 12100.
Sitlani, A., Long, E. C., Pyle, A. M., & Barton, J. K. (1992) *J. Am. Chem. Soc. 114*, 2303.
Sitlani, A. S., Dupureur, C. M., & Barton, J. K. (1993) *J. Am. Chem. Soc. 115*, 12589.
Sluka, J. P., Horvath, S. J., Bruist, M. F., Simon, M. I., & Dervan, P. B. (1987) *Science 238*, 1129.
Stubbe, J., & Kozarich, J. (1987) *Chem. Rev. 87*, 1107.
Terbreuggen, R. H., & Barton, J. K.(1995) *Biochemistry* (in press).
Tullius, T. D. (1990) *Metal–DNA Chemistry*, American Chemical Society, Washington, DC.
Wang, A. H. J., Nathans, J., van der Marel, G., van Boom, J. H., & Rich, A. (1978) *Nature 276*, 471.

BI951328L